Hindawi
Wireless Communications and Mobile Computing
Volume 2021, Article ID 2700843, 10 pages
https://doi.org/10.1155/2021/2700843

Research Article

Performance Analysis of MEC Based on NOMA under Imperfect CSI with Eavesdropper

Xuehua Li,[1,2,3] **Yingjie Pei**,[1,2,3] **Huan Jiang**,[1,2,3] **Xinwei Yue**,[1,2,3] **Yafei Wang**,[1,2,3] **and Yuqiao Suo**[4]

[1]*School of Information and Communication Engineering, Beijing Information Science and Technology University, Beijing 100101, China*
[2]*Institute of Intelligent Communication and Computing (BISTU-IICC), Beijing 100101, China*
[3]*Key Laboratory of Modern Measurement & Control Technology, Ministry of Education, Beijing 100101, China*
[4]*College of Science, Changchun University of Science and Technology, Changchun 130022, China*

Correspondence should be addressed to Huan Jiang; 18611256787@163.com

Received 19 July 2021; Revised 29 October 2021; Accepted 10 November 2021; Published 6 December 2021

Academic Editor: Xingwang Li

Mobile edge computing (MEC) is becoming more and more popular because of improving computing power in virtual reality, augmented reality, unmanned driving, and other fields. This paper investigates a nonorthogonal multiple access- (NOMA-) based MEC system, which is under imperfect channel state information (ipCSI). In this system model, a pair of users offloads their tasks to the MEC server with the existence of an eavesdropper (Eve). To evaluate the impact of Eve on the performance of the NOMA-MEC system, the secrecy outage probability (SOP) expressions for two users with the conditions of imperfect CSI and perfect channel state information (pCSI) are derived. In addition, both throughput and energy efficiency are discussed in the delay-limited transmission mode. Simulation results reveal that (1) due to the influence of channel estimation errors, the secrecy outage behaviors of two users under ipCSI conditions are worse than those of users with pCSI; (2) the secrecy performance of NOMA-MEC is superior to orthogonal multiple access- (OMA-) aided MEC systems; and (3) the NOMA-MEC systems have the ability to attain better system throughput and energy efficiency compared with OMA-MEC.

1. Introduction

As the mobile communication systems develop rapidly, the technical standards have constantly evolved. The 4th-generation communication system relies on orthogonal frequency division multiple access to operate, and the data service transmission rate reaches even 1,000 megabits per second. However, with the large-scale popularization and application of intelligent terminals, the requirements for new mobile services are increasing. The transmission rate of wireless communication will have difficulty in meeting the application requirements of future mobile communication. To improve the spectrum efficiency of the 5th-generation (5G) mobile communication technology, the industry recommends a new method of multiple access multiplexing, the nonorthogonal multiple access (NOMA). Only a single radio resource can be distributed to one user in orthogonal multiple access (OMA), while NOMA is capable of allocating one resource to multiple users at the same frequency, time, or code domain. In some scenarios like near-remote effect and large coverage multinode access cases, especially uplink communication scenarios, the nonorthogonal method with power reuse has obvious performance advantages over traditional orthogonal access.

Considerable research efforts have been devoted to investigate NOMA performance. For the downlink communications, the authors in [1] considered joint user pairing and power allocation issues, where the achievable total rate was optimized according to the minimum rate constraint of all users. To study the large cellular networks, a new analysis framework was developed to evaluate the outage performance and obtained the closed-form expressions of outage

probability [2]. The authors in [3] proposed a power allocation algorithm for a multiuser scheme to ensure successful and low-complexity successive interference cancellation (SIC) decoding and evaluated the proposed performance under different user weight ratio scenarios. As a further advance, the optimal user grouping of the downlink NOMA system was studied to make the sum rate maximal [4]. To further enhance the performance of the system, an advanced multiple-input multiple-output NOMA-aided unmanned aerial vehicle framework was proposed in [5], where the outage probability and diversity order were surveyed in depth. For the uplink communications, the authors studied the NOMA system with imperfect SIC, considered to minimize the total power consumption with the constraints of quality of service, and evaluated the impact of imperfect SIC on system performance [6]. For the cognitive Internet of Things (IoT) supporting the 6th-generation mobile communication technology, the authors of [7] proposed a hybrid spectrum access scheme based on NOMA to maximize the average data transmission rate of the cognitive IoT. The above scenarios are assumed under the ideal condition; however, the loss of distance and path is inevitable during the transmission process in actual scenarios. Thus, it is necessary to research the imperfect channel state information (ipCSI). A new method to solve the problem of multiuser detection was proposed in [8], where the receiver problem of ipCSI scenarios caused by channel estimation errors was discussed carefully. The user ending (UE) signatures presented by forward error correction channel codes under different arrangements were adopted to distinguish the desired useful signals from interfering UEs and provide robustness for channel state information (CSI) errors. Similarly, the authors of [9] designed a system model based on an ipCSI scenario, obtained the closed-form solution of the outage probability, and analyzed the performance of the NOMA system. For a cooperative NOMA system, the authors in [10] considered the influence of residual transceiver hardware damage on the system and deduced the expressions of interruption probability, traversal capacity, and energy efficiency, which proved the superiority of outage performance of cooperative NOMA. On this basis, considering the challenge of large-scale connection in IoT, the author investigated the performance of NOMA for cooperative synchronization of wireless signals and power transmission in a large-scale IoT system [11].

With the popularization of 5G, new applications have higher requirements for computing capabilities. With the core technology of mobile communication networks, mobile edge computing (MEC) sinks computing resources and storage resources closer to users and handles resource-intensive and delay-sensitive tasks at the edge of the network, which tackles the problems of extended communication resource processing time and high energy consumption. Due to the high requirements of MEC on latency and energy consumption, a mass of literature has regarded these two problems as optimization objectives. Considering the resource constraints and interference between multiple users, the authors of [12] designed an iterative MEC resource allocation algorithm which operated heuristically to make dynamic offloading decisions and confirmed that this method overmatches the cloud computing solutions in the field of execution delay and offloading efficiency. To achieve the requirements of ultra-reliability and low delay in mission-critical applications, the authors of [13] proposed a new system design, where the applications of extreme value theory to exact probability were used for local computing and task offloading. The combined application of NOMA and MEC is a pivotal solution technology. In [14], the authors comprehensively considered the uplink and downlink communication where NOMA cooperated with MEC. It indicated that NOMA-MEC can greatly reduce the delay and energy consumption of the offloading process. The authors in [15] jointly optimized the power and time distribution to cut down computing and offloading energy consumption and then obtained the closed-form expression of optimal power and time allocation solution. In [16], the partial offloading scheme based on NOMA minimized the average power consumption and realized the dynamic power delay trade-off for MEC offloading by using the Lyapunov method. To improve the offloading efficiency of edge users, a NOMA-assisted MEC system was introduced in [17], where a joint communication and computation resource iterative optimization algorithm with low complexity was proposed to minimize the energy consumption. In the full-duplex mode, edge users utilize NOMA to transfer part of the computing workload to two MEC servers. The energy consumption of the whole system was effectively reduced through the cooperation scheme, and the resources of different MEC servers were balanced to improve the experience quality of edge users. Regarding energy efficiency, the authors of [18] studied joint user association and resource allocation and proposed a matching method to reduce the energy consumption of each user in NOMA-MEC networks. It was proven that this method effectively lessens the energy consumption and iterations times. In [19], a NOMA-MEC task delay minimization problem was investigated, where a bisection search iterative algorithm is applied to tackle the nonconvex optimization issue. It is observed that the cooperation between NOMA and MEC can significantly improve energy/power efficiency.

Physical layer security (PLS) is expected to be a complementary role of wireless communication security in the future. Compared with traditional key encryption measures, PLS technology makes full use of the diversity, time variation, and heterogeneity of wireless channels to ensure that legitimate users receive private and useful information safely. Considering the existence of eavesdroppers (Eves), the author in [20] optimized the allocation of time, power, and subchannels to acquire safe and energy-saving transmission among multiple users. The authors of [21] studied the secure communications via full-duplex wiretap with wireless power supply and proposed an iterative algorithm, which was capable of achieving higher total security rate and anti-interference ability of wiretap. To enhance the security of computing task offloading, the authors in [22]

researched the security behaviors of NOMA for MEC-aware networks, considered passive eavesdropping schemes, measured the security performance of computing offload by using security interruption probability, and deduced the semiclosed form expression of the optimal solution. In order to further evaluate the eavesdropping ability of users without knowing the CSI of the Eve, the authors in [23] proposed an effective iterative algorithm to maximize the minimum antieavesdropping ability of uplink NOMA users by jointly formulating the security rate, locally calculating bits, and allocating power. To solve the delay problem of NOMA in the presence of malicious Eves, an algorithm based on binary search was proposed, which can ensure the security rate and make the maximum task delay of uplink NOMA users minimal [24]. The authors of [25] considered the transmission scenarios of single-antenna and multiantenna devices at the same time, where the exact secrecy outage probability (SOP) expressions for two antenna-aided scenarios were derived. Furthermore, the authors employed stochastic geometry to model legitimate users and Eves and studied the impact of physical layer confidentiality on the performance of a unified NOMA framework [26], where the external and internal eavesdropping scenarios were checked carefully. Given the backscatter component, the PLS of the environmental backscatter NOMA system with the actual assumptions of residuary hardware damage, channel estimation error, and imperfect SIC were studied in [27].

This paper mainly investigates the integration of NOMA and MEC by taking ipCSI and perfect channel state information (pCSI) into account, i.e., considering the Eve in the NOMA uplink-assisted MEC scenarios with channel estimation errors. The treatises of [28, 29] have studied the impact of Eves on NOMA-MEC system performance. To the best of the authors' knowledge, the NOMA-based MEC secure problem is always considered in the pCSI condition. Little is known, however, about the security performance analysis of MEC based on NOMA under ipCSI. This motivates us to evaluate the damaging influence of ipCSI for NOMA-based MEC secure communication, since pCSI is hardly obtained due to channel fading and channel estimate errors in reality. We sum up the contributions of this paper as follows:

(1) We concentrate on the secrecy performance of NOMA-MEC in the presence of an Eve. We derive the exact expressions of SOP of NOMA-MEC under ipCSI/pCSI conditions. To obtain more insights, we further derive the expressions of the asymptotic SOP at high signal-to-noise ratios (SNRs) and provide diversity orders of the legitimate user

(2) The results of system performance are also evaluated by simulation, which reveal that in the presence of the Eve, the SOP under ipCSI conditions is greater than that under the ideal condition. We also analyze the effect of channel estimation errors and the Eve's SNR on system performance. Under both ipCSI and pCSI conditions, the secrecy performance of the nearby user for NOMA-MEC overmatches that of the remote user and OMA-MEC

(3) We discuss the system throughput and energy efficiency in delay-limited transmission mode. We confirmed that NOMA-MEC is capable of attaining the greater system throughput and energy efficiency relative to OMA-MEC. As the channel estimation errors increase, the system throughput and energy efficiency of NOMA-MEC decrease seriously

2. System Model

We consider the uplink NOMA-assisted MEC communication framework as shown in Figure 1, in which the tasks are offloaded by M legitimate users to a single MEC server in the presence of an Eve, assuming that all devices are equipped with a single antenna and work in a half-duplex mode. Each link in the system experiences Rayleigh fading and will be bothered by additive white Gaussian noise (AWGN). The$n$ -th user and the$m$ -th user are selected from$M$users to offload tasks, where Eve wiretaps the communication between the users and MEC server. $\widehat{h}_i \sim \mathscr{CN}(0, \widehat{\Omega}_i)$ denotes the channel parameters of links between the user and MEC server, and $\widehat{h}_{\mathrm{Eve},i} \sim \mathscr{CN}(0, \widehat{\Omega}_{\mathrm{Eve},i})$ represents the channel parameters of links between the user and Eve, $i \in \{1, 2, \cdots, M\}$, $\widehat{\Omega}_i = \widehat{\Omega}_{\mathrm{Eve},i} = 1$.

Due to the existence of channel estimation errors, it is hard to achieve perfect CSI in actual scenarios. In order to evaluate the impact of Eve under ipCSI on the NOMA-MEC system, the channel factor of the i -th user and MEC server is modeled as $\widehat{h}_i = h_i + \varpi e_i$, and the channel parameter of the i -th user and Eve is modeled as $\widehat{h}_{\mathrm{Eve},i} = h_{\mathrm{Eve},i} + \varpi e_{\mathrm{Eve},i}$, where $\varpi \in (0, 1)$, h_i, and $h_{\mathrm{Eve},i}$ represent the channel gain under pCSI. $\varpi = 0$ represents that the system is able to acquire the pCSI, and $\varpi = 1$ represents that the system cannot acquire the pCSI and will sustain from the channel estimation error $e_i \sim \mathscr{CN}(0, \sigma_{e_i}^2)$ and $e_{\mathrm{Eve},i} \sim \mathscr{CN}(0, \sigma_{e_{\mathrm{Eve},i}}^2)$.

In this paper, the n -th and m -th users are paired to perform a nonorthogonal transmission scheme and offload their missions to the MEC server simultaneously. Moreover, the n-th/m-th user is regarded as a nearby/remote user, which is close/far to the MEC server and Eve. Therefore, the channel gains between users and the MEC server can be classified as $|h\wedge_m|^2 \le |h\wedge_n|^2$, and the channel gains between users and the Eve can be classified as $|h\wedge_{\mathrm{Eve},m}|^2 \le |h\wedge_{\mathrm{Eve},n}|^2$ [30]. According to the principle of NOMA, the received signals at the MEC server and the Eve are given by

$$y_{\mathrm{MEC}} = (h_m + \varpi e_m)\sqrt{P_m}x_m + (h_n + \varpi e_n)\sqrt{P_n}x_n + n_{\mathrm{MEC}}, \tag{1}$$

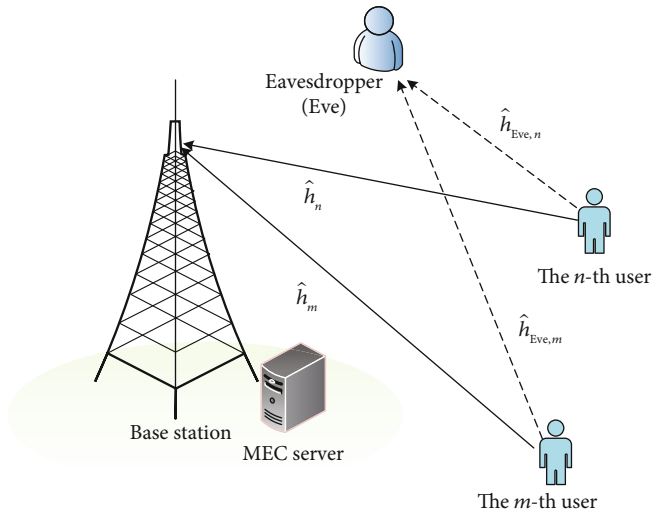

Figure 1: System model of uplink NOMA-assisted MEC communications.

$$y_{\mathrm{Eve}} = \left(h_{\mathrm{Eve},m} + \varpi e_{\mathrm{Eve},m}\right)\sqrt{P_m}x_m + \left(h_{\mathrm{Eve},n} + \varpi e_{\mathrm{Eve},n}\right)\sqrt{P_n}x_n + n_{\mathrm{Eve}}, \tag{2}$$

respectively, where x_j represents the j -th user's signal of offloading task, $j \in (m, n)$. $n_{\mathrm{MEC}} \sim \mathcal{CN}(0, \sigma^2_{\mathrm{MEC}})$ and $n_{\mathrm{Eve}} \sim \mathcal{CN}(0, \sigma^2_{\mathrm{Eve}})$ represent the AWGN at the MEC server and Eve, respectively. The transmission power of the j -th user is represented as P_j, $P_j = a_j P$, while P is the total transmission power of the paired users. In order to ensure reasonable fairness among users, we assume that $a_m > a_n$, $a_m + a_n = 1$. Hence, the signal-to-interference-plus-noise ratios (SINRs) for the MEC server to decode the information of two users are derived as

$$\gamma_n = \frac{a_n \rho |h_n|^2}{\varpi\theta_n + 1}, \tag{3}$$

$$\gamma_m = \frac{a_m \rho |h_m|^2}{a_n \rho |h_n|^2 + \varpi(\theta_n + \theta_m) + 1}, \tag{4}$$

respectively.

The SINR expressions of n -th and m -th tapped by Eve are given by

$$\gamma_{\mathrm{Eve},n} = \frac{a_n \rho_{\mathrm{Eve}} \left|h_{\mathrm{Eve},n}\right|^2}{\varpi\theta_{\mathrm{Eve},n} + 1}, \tag{5}$$

$$\gamma_{\mathrm{Eve},m} = \frac{a_m \rho_{\mathrm{Eve}} \left|h_{\mathrm{Eve},m}\right|^2}{a_n \rho_{\mathrm{Eve}} \left|h_{\mathrm{Eve},n}\right|^2 + \varpi(\theta_{\mathrm{Eve},n} + \theta_{\mathrm{Eve},m}) + 1}, \tag{6}$$

respectively, where $\rho \triangleq P/\sigma^2_{\mathrm{MEC}}$ and $\rho_{\mathrm{Eve}} \triangleq P/\sigma^2_{\mathrm{Eve}}$ represent the transmit SNR of the MEC server and Eve, $\theta_i = \sigma^2_{e_i} a_i \rho$, $\theta_{\mathrm{Eve},i} = \sigma^2_{e_{\mathrm{Eve},i}} a_i \rho_{\mathrm{Eve}}$, $i \in \{m, n\}$.

3. Performance Analysis

In this section, the secrecy outage behaviors with an Eve under ipCSI and pCSI in the uplink NOMA-MEC system are analyzed. The new exact expressions of SOP and the asymptotic SOP are derived in the high SNR region. In addition, we acquire the diversity orders and evaluate throughput as well as energy efficiency to further explore the security in NOMA-MEC.

3.1. Secrecy Outage Probability. The secrecy outage means that users cannot complete the offloading tasks within a certain time slot in the presence of the Eve. As a consequence, the secrecy outage performance for the users under the two conditions of ipCSI and pCSI with Eve is analyzed in detail.

Considering that the n -th user and the m -th user offload tasks to the MEC server at the same time, the secret rate of the two users can be defined as

$$C_n = \left[\log_2(1 + \gamma_n) - \log_2\left(1 + \gamma_{\mathrm{Eve},n}\right)\right]^+, \tag{7}$$

$$C_m = \left[\log_2(1 + \gamma_m) - \log_2\left(1 + \gamma_{\mathrm{Eve},m}\right)\right]^+, \tag{8}$$

respectively, where $(x)^+ = \max\{0, x\}$.

Assuming that the target secrecy rate of the n -th user is V_n, when its actual secrecy rate C_n is less than V_n, the n -th user has an outage behavior. Thus, the SOP of the n -th user with the ipCSI condition is expressed as

$$P_n = \Pr\left(C_n < V_n\right) = \int_0^\infty f_{\gamma_{\mathrm{Eve},n}}(x) F_{\gamma_n}\left(2^{V_n}(1 + x) - 1\right) dx. \tag{9}$$

Theorem 1. *Under the condition of ipCSI, the exact SOP expression of the n-th user in the NOMA-MEC system with*

Eve can be given by

$$P_{ipCSI}^{n} = \frac{M!}{(M-n)!(n-1)!}(\theta_{Eve,n}+1)\sum_{i=0}^{M-n}\sum_{r=0}^{n+i}\binom{M-n}{i}\binom{n+i}{r}\frac{(-1)^{i+r}}{n+i} \times e^{-\left(\left(2^{V_n}-1\right)(\varpi\theta_n+1)r/a_n\rho\Omega_n\right)}\frac{\rho\Omega_n}{(\theta_{Eve,n}+1)\rho\Omega_n+2^{V_n}(\theta_n+1)r\rho_{Eve}\Omega_{Eve,n}}, \tag{10}$$

where $\varpi = 1$.

Proof. The SINR of the n -th user in the process of offloading to the MEC server γ_n and the SINR wiretapped by Eve $\gamma_{\mathrm{Eve},n}$ can be obtained in (3) and (5), respectively. According to order statistics, the CDF of the n -th user's sorted channel gain and the PDF of the n -th user's unsorted channel gain are given by

$$F_{\gamma_n}(x) = \frac{M!}{(M-n)!(n-1)!}\sum_{i=0}^{M-n}\sum_{r=0}^{n+i}\binom{M-n}{i}\binom{n+i}{r}\frac{(-1)^{i+r}}{n+i}e^{-r(\varpi\theta_n+1)x}, \tag{11}$$

$$f_{\gamma_{\mathrm{Eve},n}}(x) = \frac{\varpi\theta_{\mathrm{Eve},n}+1}{a_n\rho_{\mathrm{Eve}}\Omega_{\mathrm{Eve},n}}e^{-((\varpi\theta_{\mathrm{Eve},n}+1)x/a_n\rho_{\mathrm{Eve}}\Omega_{\mathrm{Eve},n})}, \tag{12}$$

respectively. Substituting (11) and (12) into (9) and doing some arithmetic operations, we can get (10), which completes the proof.□ □

Corollary 2. *Upon substituting $\varpi = 0$ into (10), the exact SOP expression of the n -th user under the circumstance of pCSI with Eve is shown as*

$$P_{pCSI}^{n} = \frac{M!}{(M-n)!(n-1)!}\sum_{i=0}^{M-n}\sum_{r=0}^{n+i}\binom{M-n}{i} \cdot \binom{n+i}{r}\frac{(-1)^{i+r}}{n+i}e^{-\left(\left(2^{V_n}-1\right)r/a_n\rho\Omega_n\right)}\frac{\rho\Omega_n}{\rho\Omega_n+2^{V_n}r\rho_{Eve}\Omega_{Eve,n}}. \tag{13}$$

According to the SIC principle, the MEC server first decodes the task x_m by regarding the task x_n as an interference. By this time, a secrecy outage event occurs when the actual secrecy rate C_m is lower than the target secrecy rate $V_m = \log(1+\gamma_m)$. Therefore, the SOP under ipCSI with Eve can be given by

$$P_m = \Pr(C_m < V_m) = \int_0^{\infty} f_{\gamma_{Eve,m}}(y)F_{\gamma_m}\left(2^{V_m}(1+y)-1\right)dy. \tag{14}$$

Theorem 3. *Under the condition of ipCSI, the exact SOP expression of the m -th user with Eve is shown as*

$$P_{\mathrm{ipCSI}}^{m} = \frac{M!}{(M-m)!(m-1)!}\frac{M!}{(M-n)!(n-1)!}\sum_{i=0}^{M-m}\sum_{s=0}^{m+i}\sum_{r=0}^{M-n}\sum_{k=0}^{n+r-1}\binom{M-m}{i}\binom{m+i}{s}\binom{M-n}{r} \times \binom{n+r-1}{k}\frac{(-1)^{i+s+r+k}}{m+i}\int_0^{\infty}\left(\frac{\varpi(\theta_{\mathrm{Eve},n}+\theta_{\mathrm{Eve},m})+1}{\rho_{\mathrm{Eve}}(a_m\Omega_{\mathrm{Eve},m}+\Omega_{\mathrm{Eve},n}ya_n)}+\frac{a_na_m\Omega_{\mathrm{Eve},m}\Omega_{\mathrm{Eve},n}}{(a_m\Omega_{\mathrm{Eve},m}+\Omega_{\mathrm{Eve},n}ya_n)^2}\right) \times e^{-(y(\varpi(\theta_{\mathrm{Eve},n}+\theta_{\mathrm{Eve},m})+1)/a_m\rho_{\mathrm{Eve}}\Omega_{\mathrm{Eve},m})}e^{-\left(s\left(2^{V_m}(1+y)-1\right)[\varpi(\theta_n+\theta_m)+1]/a_m\rho\Omega_m\right)}\frac{a_m\Omega_m}{(1+k)a_m\Omega_m+s\left(2^{V_m}(1+y)-1\right)a_n\Omega_n}dy,, \tag{15}$$

where $\varpi = 1$.

Proof. See the appendix.□ □

Corollary 4. *Upon substituting $\varpi = 0$ into (15), the exact SOP expression of the m -th user under the pCSI condition with Eve can be given by*

$$P_{\mathrm{pCSI}}^{m} = \frac{M!}{(M-m)!(m-1)!}\frac{M!}{(M-n)!(n-1)!}\sum_{i=0}^{M-m}\sum_{s=0}^{m+i}\sum_{r=0}^{M-n}\sum_{k=0}^{n+r-1}\binom{M-m}{i}\binom{m+i}{s}\binom{M-n}{r} \times \binom{n+r-1}{k}\frac{(-1)^{i+s+r+k}}{m+i}\int_0^{\infty}\left(\frac{1}{\rho_{\mathrm{Eve}}(a_m\Omega_{\mathrm{Eve},m}+\Omega_{\mathrm{Eve},n}ya_n)}+\frac{a_na_m\Omega_{\mathrm{Eve},m}\Omega_{\mathrm{Eve},n}}{(a_m\Omega_{\mathrm{Eve},m}+\Omega_{\mathrm{Eve},n}ya_n)^2}\right) \times e^{-(y/a_m\rho_{\mathrm{Eve}}\Omega_{\mathrm{Eve},m})}e^{-\left(s\left(2^{V_m}(1+y)-1\right)/a_m\rho\Omega_m\right)}\frac{a_m\Omega_m}{(1+k)a_m\Omega_m+s\left(2^{V_m}(1+y)-1\right)a_n\Omega_n}dy. \tag{16}$$

3.2. Diversity Order. In this subsection, we acquire the diversity orders of users under the two CSI conditions with Eve, which is defined as follows:

$$\mu = -\lim_{\rho \longrightarrow \infty} \frac{\log\left[P^{\infty}(\rho)\right]}{\log \rho}, \tag{17}$$

where $P^{\infty}(\rho)$ denotes the SOP at high SNRs.

Corollary 5. *The asymptotic SOP of the n -th user at high SNR region under ipCSI condition with Eve is given as follows:*

$$P_{ipCSI}^{n,\infty} = \frac{M!}{(M-n)!(n-1)!}(\theta_{Eve,n}+1)\sum_{i=0}^{M-n}\sum_{r=0}^{n+i}\binom{M-n}{i}\binom{n+i}{r}\frac{(-1)^{i+r}}{n+i} \times \left(1-\frac{\left(2^{V_n}-1\right)(\theta_n+1)r}{a_n\rho\Omega_n}\right)\frac{\rho\Omega_n}{(\theta_{Eve,n}+1)\rho\Omega_n+2^{V_n}(\theta_n+1)r\rho_{Eve}\Omega_{Eve,n}}. \tag{18}$$

Remark 6. Substituting (18) into (17), the diversity order for the n -th user under ipCSI condition with Eve $\mu_{n,\mathrm{ipCSI}} = 0$ is acquired.

Corollary 7. *Substituting $\rho \longrightarrow \infty$ into (13), asymptotic SOP of the n -th user at a high SNR region under the pCSI condition with Eve is shown as*

$$P_{pCSI}^{n,\infty} = \frac{M!}{(M-n)!(n-1)!}\sum_{i=0}^{M-n}\sum_{r=0}^{n+i}\binom{M-n}{i}\binom{n+i}{r}\frac{(-1)^{i+r}}{n+i} \cdot \left(1-\frac{\left(2^{V_n}-1\right)r}{a_n\rho\Omega_n}\right)\frac{\rho\Omega_n}{\rho\Omega_n+2^{V_n}r\rho_{Eve}\Omega_{Eve,n}}. \tag{19}$$

Remark 8. Substituting (19) into (17), the diversity order for the n -th user under the pCSI condition with Eve $\mu_{n,\mathrm{pCSI}} = n$ is obtained.

3.3. Throughput Analysis. In this subsection, we discuss the system throughput in the delay-limited transmission mode of the system.

Under the condition of ipCSI, we also derive the throughput for the users with Eve, which is given by

$$R_{\mathrm{ipCSI}} = \left(1 - P_{\mathrm{ipCSI}}^{n}\right)V_n + \left(1 - P_{\mathrm{ipCSI}}^{m}\right)V_m, \tag{20}$$

where P_{ipCSI}^{n} and P_{ipCSI}^{m} have been obtained in (10) and (15), respectively.

Under the condition of pCSI, we may derive the throughput for the users with Eve, which is given by

$$R_{\mathrm{pCSI}} = \left(1 - P_{\mathrm{pCSI}}^{n}\right)V_n + \left(1 - P_{\mathrm{pCSI}}^{m}\right)V_m, \tag{21}$$

where P_{pCSI}^{n} and P_{pCSI}^{m} have been obtained in (13) and (16), respectively.

3.4. Energy Efficiency. Given the previous analysis of system throughput, we focus on the energy efficiency in NOMA-MEC in this subsection. Energy efficiency had been defined in [31].

In view of the results obtained above, the system energy efficiencies under the ipCSI and pCSI conditions with Eve are shown as

$$\eta_{\mathrm{ipCSI}} = \frac{R_{\mathrm{ipCSI}}}{TP}, \tag{22}$$

$$\eta_{\mathrm{pCSI}} = \frac{R_{\mathrm{pCSI}}}{TP}, \tag{23}$$

respectively, where T denotes the time of the whole transmission process and η_{ipCSI} and η_{pCSI} are the energy efficiency of the system under the ipCSI and pCSI conditions, respectively.

4. Results and Discussion

In this section, the simulation results verify the rationality of the theoretical expressions deduced above. The secrecy performance under the ipCSI and pCSI conditions with Eve is further evaluated seriously. We assume that the path loss factor is $\alpha = 2$ and the power allocation parameters are $a_n = 0.2$ and $a_m = 0.8$. The target secrecy rates of the users are $V_n = 2$ bits/s and $V_m = 0.05$ bits/s.

Figure 2 indicates the relationship between SOP for the two users and the transmit SNR. The channel estimation errors are set to $\sigma_{e_n}^2 = -10\,\mathrm{dB}$, $\sigma_{e_m}^2 = -10\,\mathrm{dB}$, $\sigma_{e_{\mathrm{Eve},n}}^2 = 0\,\mathrm{dB}$, and $\sigma_{e_{\mathrm{Eve},m}}^2 = -20\,\mathrm{dB}$. According to (10) and (13) and (15) and (16), the exact theoretical SOP curves of the paired users under the ipCSI and pCSI conditions with Eve are drawn, respectively. Error floors of SOP exist under the ipCSI for the NOMA-MEC system. The reason lies in the existence of interference of channel estimation errors in communication transmission. One can also observe that the error floor exists in a remote user under pCSI since the MEC server will suffer from interference of the near user while detecting the remote user's message.

As indicated in Figure 3, we study the system throughput versus SNR under ipCSI and pCSI conditions in the delay-limited transmission case with Eve. The channel estimation errors are set to $\sigma_{e_n}^2 = -10\,\mathrm{dB}$ and $\sigma_{e_m}^2 = -10\,\mathrm{dB}$. The solid curves represent the throughput in the NOMA-MEC system under ipCSI and pCSI with Eve. The dashed curves stand for the throughput in the OMA-MEC under ipCSI and pCSI with Eve. It can be observed that the throughput of NOMA-MEC under pCSI is higher than that under ipCSI. This is because the user's SOP under the pCSI condition is lower than that of the ipCSI condition, which proves that channel estimation errors and the Eve will indeed affect system performance.

Figure 4 depicts the system energy efficiency versus the SNR for the paired users under ipCSI and pCSI conditions in the delay-limited transmission case with Eve. The solid curves indicate the energy efficiency for the NOMA-MEC

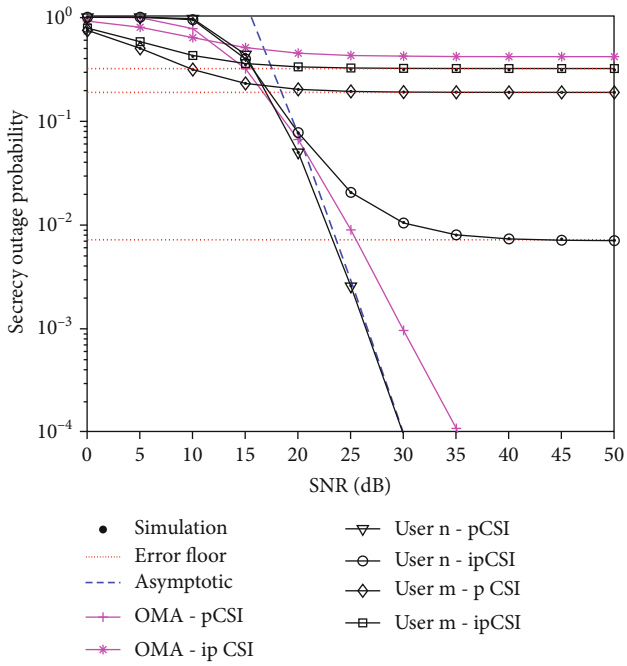

Figure 2: SOP for paired users versus SNR.

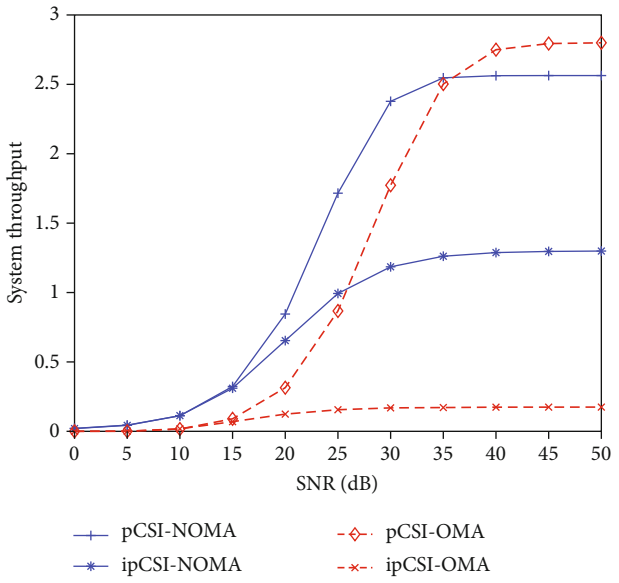

Figure 3: System throughput versus SNR in delay-limited transmission mode.

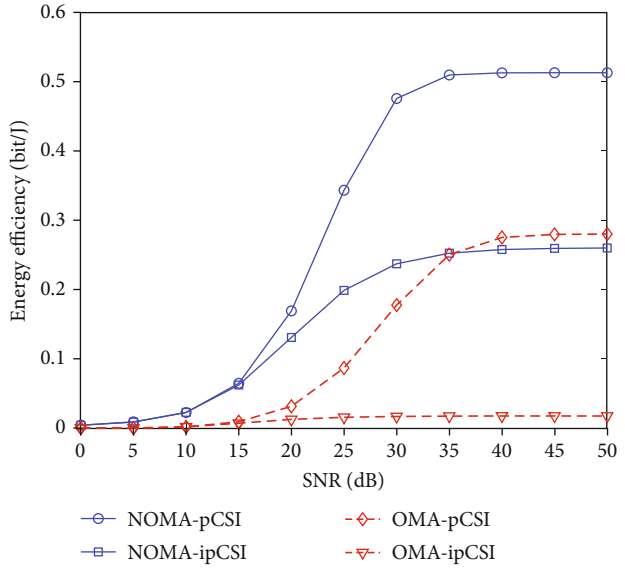

Figure 4: System energy efficiency versus SNR in delay-limited transmission mode, $P = 5$ W, and $T = 1$ s.

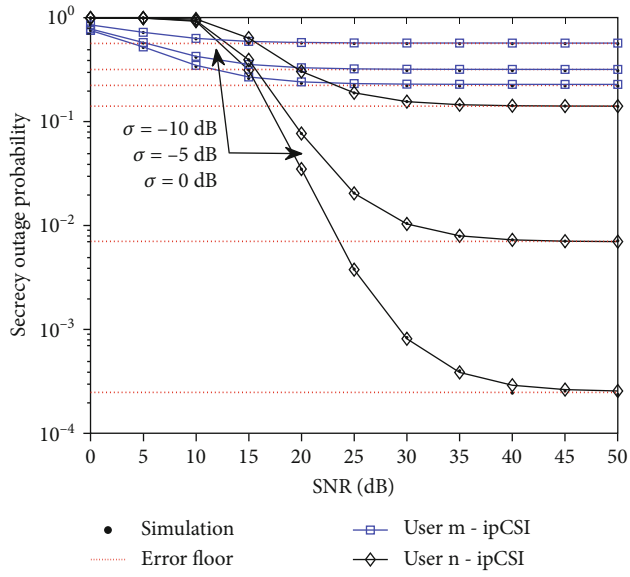

Figure 5: SOP versus SNR with different values of channel estimation errors.

system. At high SNRs, under the same conditions, NOMA-MEC obtains higher energy efficiency than OMA-MEC. Meanwhile, the energy efficiency with channel estimation error is superior to that without channel estimation error since the pCSI condition is capable of achieving much greater throughput than ipCSI condition.

In Figure 5, the SOP for the paired users with channel estimation errors from $\sigma_{e_n}^2 = \sigma_{e_m}^2 = -10$ dB to $\sigma_{e_n}^2 = \sigma_{e_m}^2 = 0$ dB is illustrated. We can observe that the quality of communication condition is improved as SNR increases. Moreover, the n-th user is closer to MEC server than the m-th user, so the improvement in SOP performance of the n-th user is much more obvious. One can also observe that the SOP rises with the increase of the channel estimation error values, and the influence on the nearby user is more obvious than the remote user on account of the interference from the nearby user, the Eve, and the channel estimation error. Meanwhile, the nearby user is only disturbed by the Eve and the channel estimation error.

Figure 6 plots the SOP for the n -th user and m -th user versus various values of target secrecy rate. When $V_m = 0.05$ bits/s, $V_n = 2$ bits/s, $V_m = 0.3$ bits/s, $V_n = 3$ bits/s, $V_m = 0.7$ bits/s, and $V_n = 4$ bits/s, it is observed that with the simultaneous increase of target secrecy rate for both users, SOP rises

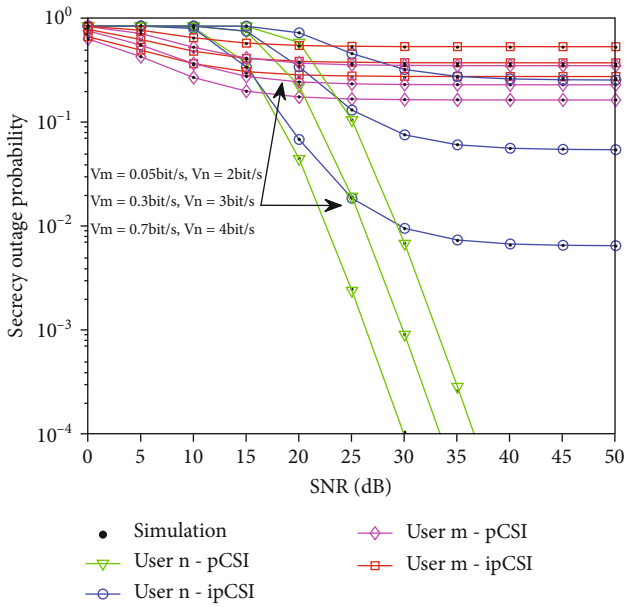

Figure 6: SOP versus SNR with various values of target secrecy rate.

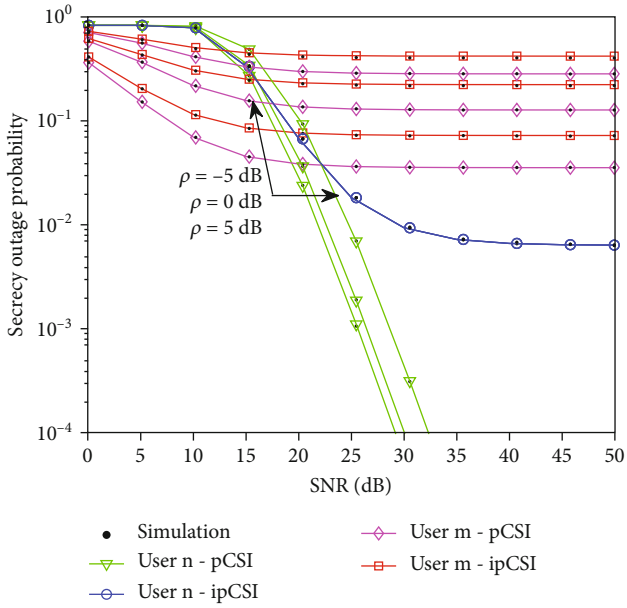

Figure 7: SOP versus SNR with different SNR values of the Eve.

as well. As a result, the influence of the target secrecy rate of users must be taken into consideration in the practical system.

Figure 7 indicates the SOP versus different SNR values of the Eve. $\rho_{\text{Eve}} = -5$ dB, $\rho_{\text{Eve}} = 0$ dB, and $\rho_{\text{Eve}} = 5$ dB. It can be seen that when the SNR values of the Eve rises, the SOP also gradually increases. That is because when the SNR of the Eve increases, it will strengthen the interference to users, which will lead to the degradation of users' secrecy performance.

5. Conclusions

We have studied the secrecy performance of uplink NOMA-MEC under ipCSI and pCSI conditions with an Eve. New exact and approximate expressions of SOP are derived for NOMA-MEC systems. The analysis results have revealed that the SOP of NOMA-MEC with pCSI performs better than that of OMA-MEC. Due to the influence of channel estimation errors, the secrecy behaviors of NOMA-MEC with ipCSI are inferior to that of pCSI. As the increase of channel estimation errors, the SOP of NOMA-MEC is getting worse. Moreover, the throughput and energy efficiency in the system have been studied under ipCSI and pCSI conditions with the Eve.

Appendix

A.1. Proof of Theorem 3

The SINR of the m -th user in the process of offloading to the MEC server γ_m and the SINR wiretapped by Eve $\gamma_{\text{Eve},m}$ can be obtained in (4) and (6), respectively. The CDF of the m -th user's unsorted channel gain is given by

$$\begin{aligned} F_{\gamma_{\text{Eve},m}}(y) &= \Pr\left(\gamma_{\text{Eve},m} < y\right) \\ &= \Pr\left(\frac{a_m \rho_{\text{Eve}} \left|h_{\text{Eve},m}\right|^2}{a_n \rho_{\text{Eve}} \left|h_{\text{Eve},n}\right|^2 + \varpi(\theta_{\text{Eve},n} + \theta_{\text{Eve},m}) + 1} < y\right) \\ &= \Pr\left(\left|h_{\text{Eve},m}\right|^2 < \frac{y\left(a_n \rho_{\text{Eve}} \left|h_{\text{Eve},n}\right|^2 + \varpi(\theta_{\text{Eve},n} + \theta_{\text{Eve},m}) + 1\right)}{a_m \rho_{\text{Eve}}}\right). \end{aligned} \tag{A.1}$$

With some simple operations, the above expression can be rewritten as

$$F_{\gamma_{\text{Eve},m}}(y) = 1 - e^{-(y(\varpi(\theta_{\text{Eve},n} + \theta_{\text{Eve},m}) + 1)/a_m \rho_{\text{Eve}} \Omega_{\text{Eve},m})} \frac{a_m \Omega_{\text{Eve},m}}{a_m \Omega_{\text{Eve},m} + \Omega_{\text{Eve},n} y a_n}. \tag{A.2}$$

Taking the derivative of (A.2), the PDF expression $f_{\gamma_{\text{Eve},m}}$ can be obtained:

$$f_{\gamma_{\text{Eve},m}}(y) = \left(\frac{\varpi(\theta_{\text{Eve},n} + \theta_{\text{Eve},m}) + 1}{\rho_{\text{Eve}}(a_m \Omega_{\text{Eve},m} + \Omega_{\text{Eve},n} y a_n)} + \frac{a_n a_m \Omega_{\text{Eve},m} \Omega_{\text{Eve},n}}{(a_m \Omega_{\text{Eve},m} + \Omega_{\text{Eve},n} y a_n)^2}\right) e^{-(y(\varpi(\theta_{\text{Eve},n} + \theta_{\text{Eve},m}) + 1)/a_m \rho_{\text{Eve}} \Omega_{\text{Eve},m})}. \tag{A.3}$$

The CDF of sorted F_{γ_m} is expressed as

$$F_{\gamma_m}(y) = \Pr(\gamma_m < y) = \Pr\left(\frac{a_m\rho|h_m|^2}{a_n\rho|h_n|^2 + \varpi(\theta_n + \theta_m) + 1} < y\right) = \Pr\left(|h_m|^2 < \frac{y\left(a_n\rho|h_n|^2 + \varpi(\theta_n + \theta_m) + 1\right)}{a_m\rho}\right). \tag{A.4}$$

Similarly, the sorted CDF expression F_{γ_m} of the m-th user can be expressed as

$$F_{\gamma_m}(y) = \frac{M!}{(M-m)!(m-1)!}\frac{M!}{(n-1)!(M-n)!}\sum_{i=0}^{M-m}\sum_{s=0}^{m+i}\sum_{r=0}^{M-n}\sum_{k=0}^{n+r-1} \cdot \binom{M-m}{i}\binom{m+i}{s} \times \binom{M-n}{r} \cdot \binom{n+r-1}{k}\frac{(-1)^{i+s+r+k}}{m+i} e^{-(sy[\varpi(\theta_n+\theta_m)+1]/a_m\rho\Omega_m)} \frac{a_m\Omega_m}{(1+k)a_m\Omega_m + sya_n\Omega_n}. \tag{A.5}$$

Substituting (A.3) and (A.5) into (14), (15) can be attained easily.

Data Availability

The data used to support the findings of this study are available from the corresponding author upon request.

Conflicts of Interest

The authors declare that they have no conflicts of interest.

Acknowledgments

This work was supported in part by the Natural Science Foundation of Beijing Municipality under Grants 4204099, L182039, and KZ201911232046; in part by the Science and Technology Project of the Beijing Municipal Education Commission under Grant KM202011232003; and in part by the Supplementary and Supportive Project for Teachers at Beijing Information Science and Technology University (2019-2021) under Grant 5111911147.

References

[1] L. Zhu, J. Zhang, Z. Xiao, X. Cao, and D. O. Wu, "Optimal user pairing for downlink non-orthogonal multiple access (NOMA)," *IEEE Wireless Communications Letters*, vol. 8, no. 2, pp. 328–331, 2019.

[2] J. Wang, B. Xia, K. Xiao, and Z. Chen, "Performance analysis and power allocation strategy for downlink NOMA systems in large-scale cellular networks," *IEEE Transactions on Vehicular Technology*, vol. 69, no. 3, pp. 3459–3464, 2020.

[3] P. Sindhu, K. S. Deepak, and K. M. Abdul Hameed, "A novel low complexity power allocation algorithm for downlink NOMA networks," in *2018 IEEE Recent Advances in Intelligent Computational Systems (RAICS)*, Thiruvananthapuram, India, 2018.

[4] J. Kang and I. Kim, "Optimal user grouping for downlink NOMA," *IEEE Wireless Communications Letters*, vol. 7, no. 5, pp. 724–727, 2018.

[5] T. Hou, Y. Liu, Z. Song, X. Sun, and Y. Chen, "Multiple antenna aided NOMA in UAV networks: a stochastic geometry approach," *IEEE Transactions on Communications*, vol. 67, no. 2, pp. 1031–1044, 2019.

[6] Z. Ming, W. Hao, O. A. Dobre, Z. Ding, and H. V. Poor, "Power minimization for multi-cell uplink NOMA with imperfect SIC," *IEEE Wireless Communications Letters*, vol. 9, no. 12, pp. 2030–2034, 2020.

[7] X. Liu, H. Ding, and S. Hu, "Uplink resource allocation for NOMA-based hybrid spectrum access in 6G-enabled cognitive internet of things," *IEEE Internet of Things Journal*, vol. 8, no. 20, pp. 15049–15058, 2021.

[8] P. Li, Z. Ding, and K. Feng, "Enhanced receiver based on FEC code constraints for uplink NOMA with imperfect CSI," *IEEE Transactions on Wireless Communications*, vol. 18, no. 10, pp. 4790–4802, 2019.

[9] S. Schiessl, M. Skoglund, and J. Gross, "NOMA in the uplink: delay analysis with imperfect CSI and finite-length coding," *IEEE Transactions on Wireless Communications*, vol. 19, no. 6, pp. 3879–3893, 2020.

[10] X. Li, J. Li, Y. Liu, Z. Ding, and A. Nallanathan, "Residual transceiver hardware impairments on cooperative NOMA networks," *IEEE Transactions on Wireless Communications*, vol. 19, no. 1, pp. 680–695, 2020.

[11] X. Li, Q. Wang, M. Liu et al., "Cooperative wireless-powered NOMA relaying for B5G IoT networks with hardware impairments and channel estimation errors," *IEEE Internet of Things Journal*, vol. 8, no. 7, pp. 5453–5467, 2021.

[12] Z. Ning, P. Dong, X. Kong, and F. Xia, "A cooperative partial computation offloading scheme for mobile edge computing enabled internet of things," *IEEE Internet of Things Journal*, vol. 6, no. 3, pp. 4804–4814, 2019.

[13] C. Liu, M. Bennis, M. Debbah, and H. V. Poor, "Dynamic task offloading and resource allocation for ultra-reliable low-latency edge computing," *IEEE Transactions on Communications*, vol. 67, no. 6, pp. 4132–4150, 2019.

[14] Z. Ding, P. Fan, and H. V. Poor, "Impact of non-orthogonal multiple access on the offloading of mobile edge computing," *IEEE Transactions on Communications*, vol. 67, no. 1, pp. 375–390, 2019.

[15] Z. Ding, J. Xu, O. A. Dobre, and H. V. Poor, "Joint power and time allocation for NOMA–MEC offloading," *IEEE Transactions on Vehicular Technology*, vol. 68, no. 6, pp. 6207–6211, 2019.

[16] N. Nouri, A. Entezari, J. Abouei, M. Jaseemuddin, and A. Anpalagan, "Dynamic power–latency tradeoff for mobile edge computation offloading in NOMA-based networks," *IEEE Internet of Things Journal*, vol. 7, no. 4, pp. 2763–2776, 2020.

[17] X. Duan, B. Li, and W. Zhao, "Energy consumption minimization for near-far server cooperation in NOMA-assisted mobile edge computing system," *IEEE Access*, vol. 8, pp. 133269–133282, 2020.

[18] G. Zheng, C. Xu, and L. Tang, "Joint user association and resource allocation for NOMA-based MEC: a matching-coalition approach," in *2020 IEEE Wireless Communications and Networking Conference (WCNC)*, Seoul, Korea (South), 2020.

[19] F. Fang, Y. Xu, Z. Ding, C. Shen, M. Peng, and G. K. Karagiannidis, "Optimal resource allocation for delay minimization in NOMA-MEC networks," *IEEE Transactions on Communications*, vol. 68, no. 12, pp. 7867–7881, 2020.

[20] L. Lei, Z. Chang, Y. Hu, T. Ristaniemi, Y. Yuan, and S. Chatzinotas, "Energy-efficient resource optimization with wireless power transfer for secure NOMA systems," in *2018 IEEE/CIC International Conference on Communications in China (ICCC)*, Beijing, China, 2018.

[21] Q. Li and D. Xu, "Secure communication with a wireless powered full-duplex eavesdropper," in *2019 IEEE 19th International Conference on Communication Technology (ICCT)*, Xi'an, China, 2019.

[22] W. Wu, F. Zhou, R. Q. Hu, and B. Wang, "Energy-efficient resource allocation for secure NOMA-enabled mobile edge computing networks," *IEEE Transactions on Communications*, vol. 68, no. 1, pp. 493–505, 2020.

[23] W. Wu, X. Wang, F. Zhou, K. Wong, C. Li, and B. Wang, "Resource allocation for enhancing offloading security in NOMA-enabled MEC networks," *IEEE Systems Journal (Early Access)*, vol. 15, pp. 1–4, 2020.

[24] X. Wang, W. Wu, B. Lyu, and H. Wang, "Delay minimization for secure NOMA mobile-edge computing," in *2019 IEEE 19th International Conference on Communication Technology (ICCT)*, Xi'an, China, 2019.

[25] Y. Liu, Z. Qin, M. Elkashlan, Y. Gao, and L. Hanzo, "Enhancing the physical layer security of non-orthogonal multiple access in large-scale networks," *IEEE Transactions on Wireless Communications*, vol. 16, no. 3, pp. 1656–1672, 2017.

[26] X. Yue, Y. Liu, Y. Yao, X. Li, R. Liu, and A. Nallanathan, "Secure communications in a unified non-orthogonal multiple access framework," *IEEE Transactions on Wireless Communications*, vol. 19, no. 3, pp. 2163–2178, 2020.

[27] X. Li, M. Zhao, M. Zeng et al., "Hardware impaired ambient backscatter NOMA systems: reliability and security," *IEEE Transactions on Communications*, vol. 69, no. 4, pp. 2723–2736, 2021.

[28] W. Wu, F. Zhou, P. Li, P. Deng, B. Wang, and V. C. M. Leung, "Energy-efficient secure NOMA-enabled mobile edge computing networks," in *ICC 2019-2019 IEEE International Conference on Communications (ICC)*, Shanghai, China, 2019.

[29] H. Jiang, Y. Wang, X. Yue, and X. Li, "Performance analysis of NOMA-based mobile edge computing with imperfect CSI," *EURASIP Journal on Wireless Communications and Networking*, vol. 2020, no. 1, 2020.

[30] H. A. David and H. N. Nagaraja, *Order Statistics*, Wiley, New York, NY, USA, 3rd edition, 2003.

[31] X. Yue, Y. Liu, S. Kang, A. Nallanathan, and Z. Ding, "Exploiting full/half-duplex user relaying in NOMA systems," *IEEE Transactions on Communications*, vol. 66, no. 2, pp. 560–575, 2018.